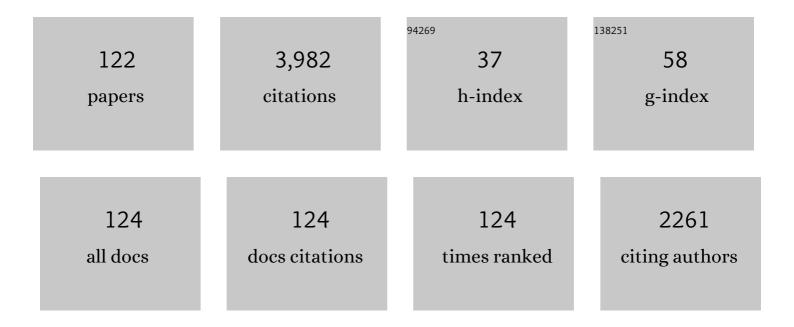
Akio Suzuki

List of Publications by Year in descending order

Source: https://exaly.com/author-pdf/5790629/publications.pdf Version: 2024-02-01



Δείο Suzuri

#	Article	IF	CITATIONS
1	Stability of hydrous melt at the base of the Earth's upper mantle. Nature, 2006, 439, 192-194.	13.7	165
2	Viscosity of peridotite liquid up to 13 GPa: Implications for magma ocean viscosities. Earth and Planetary Science Letters, 2005, 240, 589-604.	1.8	144
3	Ponded melt at the boundary between the lithosphere and asthenosphere. Nature Geoscience, 2013, 6, 1041-1044.	5.4	144
4	A new hydrous phase δ-AlOOH synthesized at 21 GPa and 1000 °C. Physics and Chemistry of Minerals, 2000, 27, 689-693.	0.3	134
5	Stability of dense hydrous magnesium silicate phases and water storage capacity in the transition zone and lower mantle. Physics of the Earth and Planetary Interiors, 2001, 124, 105-117.	0.7	125
6	In situ determination of the phase boundary between Wadsleyite and Ringwoodite in Mg2SiO4. Geophysical Research Letters, 2000, 27, 803-806.	1.5	121
7	Effect of structural transitions on properties of high-pressure silicate melts: 27Al NMR, glass densities, and melt viscosities. American Mineralogist, 2007, 92, 1093-1104.	0.9	111
8	In situ X-ray diffraction study of post-spinel transformation in a peridotite mantle: Implication for the 660-km discontinuity. Earth and Planetary Science Letters, 2005, 238, 311-328.	1.8	108
9	Wet subduction versus cold subduction. Geophysical Research Letters, 2005, 32, .	1.5	104
10	Stability field of new hydrous phase, δ-AlOOH, with implications for water transport into the deep mantle. Geophysical Research Letters, 2001, 28, 3991-3993.	1.5	91
11	The viscosity of CaMgSi2O6 liquid at pressures up to 13GPa. Physics of the Earth and Planetary Interiors, 2003, 139, 45-54.	0.7	87
12	Viscosity of albite melt at high pressure and high temperature. Physics and Chemistry of Minerals, 2002, 29, 159-165.	0.3	81
13	Melting relations of peridotite and the density crossover in planetary mantles. Chemical Geology, 1995, 120, 207-221.	1.4	77
14	Density of peridotite melts at high pressure. Physics and Chemistry of Minerals, 2003, 30, 449-456.	0.3	73
15	Thermal history of the enstatite chondrites from silica polymorphs. Meteoritics and Planetary Science, 2005, 40, 855-868.	0.7	68
16	Flotation of Diamond in Mantle Melt at High Pressure. Science, 1995, 269, 216-218.	6.0	66
17	Measurement of hydrous peridotite magma density at high pressure using the X-ray absorption method. Earth and Planetary Science Letters, 2009, 287, 293-297.	1.8	63
18	The effect of temperature, pressure, and sulfur content on viscosity of the Fe–FeS melt. Earth and Planetary Science Letters, 2001, 190, 93-101.	1.8	61

#	Article	IF	CITATIONS
19	Effect of water in depleted mantle on post-spinel transition and implication for 660 km seismic discontinuity. Earth and Planetary Science Letters, 2013, 371-372, 103-111.	1.8	60
20	Density and thermal expansion of a peridotite melt at high pressure. Physics of the Earth and Planetary Interiors, 1998, 107, 53-61.	0.7	57
21	Mechanisms and kinetics of the post-spinel transformation in Mg2SiO4. Physics of the Earth and Planetary Interiors, 2002, 129, 153-171.	0.7	56
22	Stability of carbonated magmas at the base of the Earth's upper mantle. Geophysical Research Letters, 2007, 34, .	1.5	55
23	Kushiroite, CaAlAlSiO6: A new mineral of the pyroxene group from the ALH 85085 CH chondrite, and its genetic significance in refractory inclusions. American Mineralogist, 2009, 94, 1479-1482.	0.9	54
24	Symmetrization driven spin transition in ε-FeOOH at high pressure. Earth and Planetary Science Letters, 2013, 379, 49-55.	1.8	54
25	In situ X ray observation of high-pressure phase transitions of MgSiO3and thermal expansion of MgSiO3perovskite at 25 GPa by double-stage multianvil system. Journal of Geophysical Research, 1995, 100, 20475-20481.	3.3	51
26	Diamond-Graphite Relationships in Ultrahigh-pressure Metamorphic Rocks from the Kokchetav Massif, Northern Kazakhstan. Journal of Petrology, 2010, 51, 763-783.	1.1	51
27	Absence of density crossover between basalt and peridotite in the cold slabs passing through 660 km discontinuity. Geophysical Research Letters, 2004, 31, .	1.5	50
28	Stability of Fe–Ni hydride after the reaction between Fe–Ni alloy and hydrous phase (l̂´-AlOOH) up to 1.2Mbar: Possibility of H contribution to the core density deficit. Physics of the Earth and Planetary Interiors, 2012, 194-195, 18-24.	0.7	50
29	Dislocation-accommodated grain boundary sliding as the major deformation mechanism of olivine in the Earth's upper mantle. Science Advances, 2015, 1, e1500360.	4.7	49
30	Pressure-volume-temperature equation of state of tungsten carbide to 32 GPa and 1673 K. Journal of Applied Physics, 2010, 108, .	1.1	48
31	Transformation textures, mechanisms of formation of highâ€pressure minerals in shock melt veins of L6 chondrites, and pressureâ€ŧemperature conditions of the shock events. Meteoritics and Planetary Science, 2009, 44, 1771-1786.	0.7	46
32	Hydrogen partitioning between iron and ringwoodite: Implications for water transport into the Martian core. Earth and Planetary Science Letters, 2009, 287, 463-470.	1.8	44
33	Viscosity of silicate melts in CaMgSi2O6–NaAlSi2O6 system at high pressure. Physics and Chemistry of Minerals, 2005, 32, 140-145.	0.3	43
34	Density of dry peridotite magma at high pressure using an X-ray absorption method. American Mineralogist, 2010, 95, 144-147.	0.9	43
35	The effect of sulfur content on density of the liquid Fe–S at high pressure. Physics and Chemistry of Minerals, 2008, 35, 417-423.	0.3	42
36	Chemical Reactions Between Fe and H ₂ 0 up to Megabar Pressures and Implications for Water Storage in the Earth's Mantle and Core. Geophysical Research Letters, 2018, 45, 1330-1338.	1.5	42

#	Article	IF	CITATIONS
37	Density measurement of Fe ₃ C liquid using Xâ€ray absorption image up to 10 GPa and effect of light elements on compressibility of liquid iron. Journal of Geophysical Research, 2010, 115, .	3.3	40
38	Viscosity of the albite melt to 7 GPa at 2000 K. Earth and Planetary Science Letters, 2000, 175, 87-92.	1.8	39
39	Effect of pressure on the viscosity of Fe-S and Fe-C liquids up to 16 GPa. Geophysical Research Letters, 2006, 33, .	1.5	36
40	Formation of metastable assemblages and mechanisms of the grain-size reduction in the Postspinel transformation of Mg2SiO4. Geophysical Research Letters, 2000, 27, 807-810.	1.5	35
41	Density of high-Ti basalt magma at high pressure and origin of heterogeneities in the lunar mantle. Earth and Planetary Science Letters, 2010, 299, 285-289.	1.8	35
42	Pressure and temperature dependence of the viscosity of a NaAlSi2O6 melt. Physics and Chemistry of Minerals, 2011, 38, 59-64.	0.3	35
43	Radiographic study on the viscosity of the Fe-FeS melts at the pressure of 5 to 7 GPa. American Mineralogist, 2001, 86, 578-582.	0.9	34
44	Melting relations of hydrous and dry mantle compositions and the genesis of komatiites. Geophysical Research Letters, 1998, 25, 2201-2204.	1.5	33
45	High-pressure X-ray diffraction study of ε-FeOOH. Physics and Chemistry of Minerals, 2010, 37, 153-157.	0.3	33
46	Density measurement of liquid FeS at high pressures using synchrotron X-ray absorption. American Mineralogist, 2011, 96, 864-868.	0.9	33
47	Viscosity change and structural transition of Molten Fe at 5 GPa. Geophysical Research Letters, 2002, 29, 68-1-68-3.	1.5	32
48	Density of Fe-3.5 wt% C liquid at high pressure and temperature and the effect of carbon on the density of the molten iron. Physics of the Earth and Planetary Interiors, 2013, 224, 77-82.	0.7	31
49	Towards a consensus on the pressure and composition dependence of sound velocity in the liquid Feâ \in S system. Physics of the Earth and Planetary Interiors, 2016, 257, 230-239.	0.7	31
50	Yamato 792947, 793408 and 82038: The most primitive H chondrites, with abundant refractory inclusions. Meteoritics and Planetary Science, 2002, 37, 1417-1434.	0.7	30
51	Thermal equation of state of superhydrous phase B to 27GPa and 1373K. Physics of the Earth and Planetary Interiors, 2007, 164, 142-160.	0.7	30
52	Intrusion of UHP metamorphic rocks into the upper crust of Kyrgyzian Tien-Shan: P-T path and metamorphic age of the Makbal Complex. Journal of Mineralogical and Petrological Sciences, 2010, 105, 233-250.	0.4	29
53	In situviscosity measurements of albite melt under high pressure. Journal of Physics Condensed Matter, 2002, 14, 11343-11347.	0.7	27
54	The compressibility of Fe- and Al-bearing phase D to 30ÂGPa. Physics and Chemistry of Minerals, 2007, 34, 159-167.	0.3	27

#	Article	IF	CITATIONS
55	Density measurements of liquid Fe–Si alloys at high pressure using the sink–float method. Physics and Chemistry of Minerals, 2011, 38, 801-807.	0.3	27
56	High-temperature viscosity measurements of hydrous albite liquid using in-situ falling-sphere viscometry at 2.5 GPa. Chemical Geology, 2006, 229, 2-9.	1.4	25
57	Flotation of Olivine in the Peridotite Melt at High Pressure Proceedings of the Japan Academy Series B: Physical and Biological Sciences, 1993, 69, 23-28.	1.6	24
58	An in situ X ray diffraction study of the α-β transformation kinetics of Mg2SiO4. Geophysical Research Letters, 1998, 25, 695-698.	1.5	24
59	Stability field of phase Egg, AlSiO ₃ OH at high pressure and high temperature: possible water reservoir in mantle transition zone. Journal of Mineralogical and Petrological Sciences, 2017, 112, 31-35.	0.4	24
60	The high-pressure and temperature equation of state of a majorite solid solution in the system of Mg 4 Si 4 O 12 -Mg 3 Al 2 Si 3 O 12. Physics and Chemistry of Minerals, 1999, 27, 3-10.	0.3	23
61	Thermal equation of state of Al―and Feâ€bearing phase D. Journal of Geophysical Research, 2008, 113, .	3.3	23
62	In situ measurement of interfacial tension of Fe–S and Fe–P liquids under high pressure using X-ray radiography and tomography techniques. Physics of the Earth and Planetary Interiors, 2009, 174, 220-226.	0.7	23
63	Space group and hydrogen sites of ?-AlOOH and implications for a hypothetical high-pressure form of Mg(OH)2. Physics and Chemistry of Minerals, 2004, 31, 360.	0.3	22
64	Compressional behavior and spin state of δ-(Al,Fe)OOH at high pressures. American Mineralogist, 2019, 104, 1273-1284.	0.9	22
65	Neutron diffraction study of aluminous hydroxide δ-AlOOD. Physics and Chemistry of Minerals, 2007, 34, 657-661.	0.3	21
66	Compressibility of the high-pressure polymorph of AlOOH to 17 GPa. Mineralogical Magazine, 2009, 73, 479-485.	0.6	20
67	Flotation of olivine and diamond in mantle melt at high pressure: Implications for fractionation in the deep mantle and ultradeep origin of diamond. Geophysical Monograph Series, 1998, , 227-239.	0.1	18
68	Neutron diffraction study of hydrous phase G: Hydrogen in the lower mantle hydrous silicate, phase G. Geophysical Research Letters, 2001, 28, 3987-3990.	1.5	18
69	Single crystal synthesis of δ-(Al,Fe)OOH. American Mineralogist, 2017, 102, 1953-1956.	0.9	18
70	Viscosity of liquid sulfur under high pressure. Journal of Physics Condensed Matter, 2004, 16, 1707-1714.	0.7	17
71	Superplasticity in hydrous melt-bearing dunite: Implications for shear localization in Earth's upper mantle. Earth and Planetary Science Letters, 2012, 335-336, 59-71.	1.8	17
72	Speciation of and D/H partitioning between fluids and melts in silicate-D-O-H-C-N systems determined in-situ at upper mantle temperatures, pressures, and redox conditions. American Mineralogist, 2014, 99, 578-588.	0.9	17

#	Article	IF	CITATIONS
73	In situ observation of crystallographic preferred orientation of deforming olivine at high pressure and high temperature. Physics of the Earth and Planetary Interiors, 2015, 243, 1-21.	0.7	17
74	Designing PLANET: Neutron beamline for high-pressure material science at J-PARC. Journal of Physics: Conference Series, 2010, 215, 012025.	0.3	15
75	P–V–T equation of state of Na-majorite to 21 GPa and 1673 K. Physics of the Earth and Planetary Interiors, 2014, 227, 68-75.	0.7	15
76	Pressure–volume–temperature equation of state of ε–FeOOH to 11 GPa and 700 K. Journal of Mineralogical and Petrological Sciences, 2016, 111, 420-424.	0.4	15
77	In situ observation and determination of liquid immiscibility in the Feâ€Oâ€S melt at 3 GPa using a synchrotron Xâ€ray radiographic technique. Geophysical Research Letters, 2007, 34, .	1.5	14
78	Rheology of fineâ€grained forsterite aggregate at deep upper mantle conditions. Journal of Geophysical Research: Solid Earth, 2014, 119, 253-273.	1.4	14
79	Effect of sulfur on sound velocity of liquid iron under Martian core conditions. Nature Communications, 2020, 11, 1954.	5.8	13
80	The influence of δ-(Al,Fe)OOH on seismic heterogeneities in Earth's lower mantle. Scientific Reports, 2021, 11, 12036.	1.6	12
81	Thermoelastic properties of chromium oxide Cr2O3 (eskolaite) at high pressures and temperatures. Physics and Chemistry of Minerals, 2016, 43, 447-458.	0.3	11
82	Viscosity and density measurements of melts and glasses at high pressure and temperature by using the multi-anvil apparatus and synchrotron X-ray radiation. , 2005, , 195-209.		10
83	Thermal equation of state of majoritic knorringite and its significance for continental upper mantle. Journal of Geophysical Research: Solid Earth, 2014, 119, 8034-8046.	1.4	10
84	Structure and Density of H ₂ Oâ€Rich Mg ₂ SiO ₄ Melts at High Pressure From Ab Initio Simulations. Journal of Geophysical Research: Solid Earth, 2020, 125, e2020JB020365.	1.4	10
85	Compression behavior of manganite. Journal of Mineralogical and Petrological Sciences, 2013, 108, 295-299.	0.4	9
86	In situ X–ray diffraction studies of hydrous aluminosilicate at high pressure and temperature. Journal of Mineralogical and Petrological Sciences, 2018, 113, 106-111.	0.4	9
87	Sound velocity measurements of ε–FeOOH up to 24 GPa. Journal of Mineralogical and Petrological Sciences, 2019, 114, 155-160.	0.4	9
88	Hydrous magnesium-rich magma genesis at the top of the lower mantle. Scientific Reports, 2019, 9, 7420.	1.6	9
89	Effects of alkali and alkaline-earth cations on the high-pressure sound velocities of aluminosilicate glasses. Physics and Chemistry of Minerals, 2020, 47, 1.	0.3	8
90	Deformation cubic anvil press and stress and strain measurements using monochromatic X-rays at high pressure and high temperature. High Pressure Research, 2011, 31, 399-406.	0.4	7

#	Article	IF	CITATIONS
91	Thermal equation of state of goethite (α-FeOOH). High Pressure Research, 2017, 37, 193-199.	0.4	7
92	Flow behavior and microstructures of hydrous olivine aggregates at upper mantle pressures and temperatures. Contributions To Mineralogy and Petrology, 2017, 172, 1.	1.2	7
93	Effect of carbon dioxide on the viscosity of a melt of jadeite composition at high pressure. Journal of Mineralogical and Petrological Sciences, 2018, 113, 47-50.	0.4	6
94	On the origin of the Kamiokande experiment and neutrino astrophysics. European Physical Journal H, 2012, 37, 33-73.	0.5	5
95	Pressure–induced structural changes of basaltic glass. Journal of Mineralogical and Petrological Sciences, 2018, 113, 286-292.	0.4	5
96	Elastic properties and structures of pyrope glass under high pressures. American Mineralogist, 2021, 106, 7-14.	0.9	5
97	The 20th anniversary of SN1987A. Journal of Physics: Conference Series, 2008, 120, 072001.	0.3	4
98	Corrigendum to "Effect of water in depleted mantle on post-spinel transition and implication for 660 km seismic discontinuity―[Earth Planet. Sci. Lett. 371–372 (2013) 103–111]. Earth and Planetary Science Letters, 2013, 382, 85-86.	1.8	4
99	Application of X-ray radiography to study the segregation process of iron from silicate under high pressure and high temperature. High Pressure Research, 2015, 35, 130-138.	0.4	4
100	<i>P–V–T</i> equation of state of rhodium oxyhydroxide. High Pressure Research, 2018, 38, 145-152.	0.4	4
101	The sound velocity of wüstite at high pressures: implications for low-velocity anomalies at the base of the lower mantle. Progress in Earth and Planetary Science, 2020, 7, .	1.1	4
102	In Situ X Ray Observation of the Phase Transitions from .ALPHA. to .GAMMA. and from .GAMMA. to Perovskite+Periclase in Mg2SiO4 Review of High Pressure Science and Technology/Koatsuryoku No Kagaku To Gijutsu, 1998, 7, 119-121.	0.1	4
103	Phase relationships of the system Fe-Ni-S and structure of the high-pressure phase of (Fe1â^'xNix)3S2. Physics of the Earth and Planetary Interiors, 2018, 277, 30-37.	0.7	3
104	The stability of anhydrous phase B, Mg14Si5O24, at mantle transition zone conditions. Physics and Chemistry of Minerals, 2018, 45, 523-531.	0.3	3
105	Do SnI ₄ molecules deform on heating and pressurization in the low-pressure crystalline phase?. Journal of Physics Condensed Matter, 2020, 32, 055401.	0.7	3
106	In situ observation of the pyroxene-majorite transition in Na2MgSi5O12 using synchrotron radiation and Raman spectroscopy of Na-majorite. American Mineralogist, 2015, 100, 378-384.	0.9	2
107	In-situ X-ray diffraction study on β-CrOOH at high pressure and high-temperature. High Pressure Research, 2019, 39, 499-508.	0.4	2
108	Structure of basaltic glass at pressures up to 18 GPa. American Mineralogist, 2022, 107, 325-335.	0.9	2

#	Article	IF	CITATIONS
109	Phase transitions of ScOOH under high pressure. High Pressure Research, 2021, 41, 275-289.	0.4	2
110	High Pressure Earth Science. Physical Properties of Silicate Melt at High Pressure Review of High Pressure Science and Technology/Koatsuryoku No Kagaku To Gijutsu, 1999, 9, 11-18.	0.1	2
111	Creep behavior during the eutectoid transformation of albite: Implications for the slab deformation in the lower mantle. Earth and Planetary Science Letters, 2014, 388, 92-97.	1.8	1

112 āfžāf«āfā,¢āf³āf"āf«ā,'ç""ā,āŸé«~æ,©é«~圧実é"" —最èį'ã®æ^œžœâ€". Ganseki Kobutsu Kagaku, 2001, 301, 102-103.

113	Micro-Raman spectroscopy of small crystals Ganseki Kobutsu Kagaku, 2001, 30, 241-246.	0.1	1
114	Density and Viscosity of Magma and Metallic Liquid at High Pressures and Temperatures. Review of High Pressure Science and Technology/Koatsuryoku No Kagaku To Gijutsu, 2005, 15, 146-155.	0.1	1
115	Viscosity of melt of soda melilite composition at high pressure. Journal of Mineralogical and Petrological Sciences, 2019, 114, 41-44.	0.4	1
116	High Pressure Experiments and the Study of the Earth's Interior. Review of High Pressure Science and Technology/Koatsuryoku No Kagaku To Gijutsu, 2007, 17, 198-205.	0.1	0
117	Preface for the article collection "High-Pressure Earth and Planetary Science in the last and next decade― Progress in Earth and Planetary Science, 2016, 3, .	1.1	0
118	A unique multianvil 6–6 assembly for a cubic-type multianvil apparatus. Review of Scientific Instruments, 2021, 92, 025117.	0.6	0
119	Viscosity of K ₂ TiSi ₄ O ₁₁ melt at high pressure. Journal of Mineralogical and Petrological Sciences, 2019, 114, 280-283.	0.4	0
120	Localized Deformation of Lawsonite During Cold Subduction. Journal of Geophysical Research: Solid Earth, 2022, 127, .	1.4	0
121	In situ X–ray diffraction study of the phase boundary between diaspore and δ–AlOOH. Journal of Mineralogical and Petrological Sciences, 2022, 117, n/a.	0.4	0
122	<i>P</i> - <i>V</i> - <i>T</i> equation of state of α-ScOOH High Pressure Research, 0, , 1-13.	0.4	0